

**Analysis of surface wind diurnal cycle in tropical region
using mooring observations and CCMP product**

Xiaochun Wang^{a,*} Kefeng Zhu^b C.K. Shum^b Joel Johnson^c

May 5, 2014

Extended abstract for 31 AMS Tropical Meteorology and Hurricane Meeting
Paper Number 7A.7

^aXiaochun Wang, JIFRESSE, Univ. of California at Los Angeles, Los Angeles, CA
90095, E-mail: xcwang@jifresse.ucla.edu

^bDivision of Geodetic Sciences, School of Earth Sciences, The Ohio State University,
Columbus, OH

^cDepartment of Electrical and Computer Engineering and ElectroScience Labora-
tory, The Ohio State University, Columbus, OH

Abstract

The diurnal cycle of ocean surface wind and its convergence were analyzed using available tropical mooring observations from TAO, PIRATA and RAMA programs and a gridded ocean surface wind product, Cross-Calibrated Multi-Platform Ocean Surface Wind Velocity (CCMP), which is a blended product using available satellite surface wind observations and ECMWF analysis. The objectives of our study are to assess the fidelity of CCMP product and the variability of surface wind and its convergence at diurnal frequency band, and to apply to the analysis of wind observation from future satellite missions, including the Cyclonic Global Navigation Satellite System (CYGNSS) mission. With an 8-microsatellite constellation, the CYGNSS mission is designed to measure ocean surface wind field with a mean revisit time of 4 hours between 35N and 35S and through all levels of precipitation events. Our analysis period is from 2002 to 2011, during which there were at least six satellites that could provide observations. The Root Mean Square Difference (RMSD) of hourly wind between CCMP wind and tropical mooring observation is around $1 - 2 \text{ m s}^{-1}$ or 30% of the total wind speed and with significantly high correlations, indicating the fidelity of CCMP product. The discrepancies between CCMP wind and mooring observation tend to be larger during precipitating periods. Regions of large variability of wind and its convergence at diurnal frequency band are the coast region, central part of subtropical highs. The ITCZ and SPCZ regions also show up clearly in the variability of wind and its convergence at diurnal frequency band.

1 Introduction

Diurnal cycle is one of the strongest natural modes in Earth system. Many atmospheric parameters in tropical regions have significant diurnal cycle signal. Precipitation and the amount of deep convective clouds have significant diurnal cycle (e.g., Yang and Slingo 2001; Tian et al. 2006) and also interact with variability at longer time scales (Oh et al. 2012). The diurnal cycle of surface wind, however, is not studied extensively. Deser and Smith (1998) has analyzed the diurnal cycle of wind using mooring wind observations and quantified the magnitude of diurnal cycle of wind. However, their analysis is based on sparse observations. In present research, the magnitude of surface wind diurnal cycle is studied using a gridded product by blending surface wind analysis from ECMWF and satellite wind speed and wind vector observations. Our motivations are to assess the quality of the gridded ocean surface wind product and to quantify the magnitude of surface wind diurnal cycle on global scale.

The Cyclone Global Navigation Satellite System (CYGNSS) is designed to observe ocean surface wind observation from 35S to 35N with an averaged revisit time of 4hr and for all levels of precipitation events. Our study prepares for the potential applications of CYGNSS wind product in terms of potential interaction among variability at different time scales.

2 Data

The gridded ocean surface wind used in present study is the Cross-Calibrated Multi-Platform (CCMP) Ocean Surface Wind Velocity, which combines surface wind analysis from ECMWF and wind speed observations from SSM/I, AMSRE, and TMI and ocean surface wind vector observations from QuikSCAT and SeaWinds. An enhanced variational method was used to blend satellite surface wind observation

and the 10m winds from ECMWF (Atlas et al. 1996; Hoffman et al. 2003). The ERA-40 Reanalysis was used as a background field for the period from July 1987 to December 1998. Beginning in 1999, the ECMWF operational analysis was used as background. Since 2002 there were at least six satellites that can provide wind observation. Mooring stations in the tropical Pacific started to provide hourly (or higher frequency) surface wind observation since 1980s (McPhaden et al. 1998). Gradually the mooring arrays were extended to the tropical Atlantic (Servain et al. 1998; Boules et al. 2008) and the tropical Indian Ocean (McPhaden 2009). Mainly based on the above consideration, our analysis is for the period from 2002 to 2011. Surface wind observations from 108 stations were used, with missing periods from time to time. It should be noted than no extra quality control procedure was conducted for in situ mooring observations. The quality controlled data from PMEL/NOAA were used in our analysis.

3 Results

3.1 Comparison of CCMP and mooring observation

Hourly wind observations from mooring arrays were compared with CCMP wind by bilinearly interpolating CCMP wind to station location and matching time. Figure 1 is a typical example of the comparison, indicating the Root-Mean-Square Difference (RMSD) between CCMP zonal wind and mooring observations at 0N, 147E is around 1 m s^{-1} , and with high correlation coefficient around 0.95. Since the hourly observation is used, the RMSD is higher than that of Atlas et al. (2003) which used monthly averaged wind.

The comparison was conducted from 2002 to 2011 and all the mooring observations from 108 stations were used. Figure 2 is the averaged RMSD of wind between mooring observation and CCMP wind interpolated to mooring locations. The RMSD

of wind (W_{RMSD}) is defined as

$$W_{RMSD} = (U_{RMSD}^2 + V_{RMSD}^2)^{1/2}, \quad (1)$$

in which U_{RMSD} and V_{RMSD} is the RMSD for zonal and meridional wind component, respectively. When there are more than 120 wind observations available, W_{RMSD} is computed for the particular station for that year. Figure 2 is the averaged W_{RMSD} from 2002 to 2011. The W_{RMSD} is generally between 1-2 $m s^{-1}$ and regions associated with high precipitation such as ITCZ regions of the Pacific and Atlantic, SPCZ, and the eastern Indian Ocean have higher W_{RMSD} than low precipitation regions such as Eastern Pacific and Eastern Atlantic. The high W_{RMSD} in precipitation regions is presumably caused by the effect of rain on the microwave instruments commonly used by current satellite missions. The CYGNSS mission will use L-band and can observe ocean surface wind for all precipitation events, whose advantage needs to be evaluated after its launch in 2016.

Figure 3 shows the change of W_{RMSD} from 2002 to 2011. The W_{RMSD} varies between 1.6-1.8 $m s^{-1}$. The W_{RMSD} is about 25-30% of the total wind speed in tropical regions (low panel of Figure 3). If the comparison is separated into precipitating (hourly rain rate greater than 0.01 $mm hr^{-1}$) and non-precipitating time (hourly rain rate smaller than 0.01 $mm hr^{-1}$) (Figure 4), W_{RMSD} for precipitating time is generally higher by about 0.2 $m s^{-1}$.

3.2 Surface wind diurnal cycle

Power spectrum analysis was conducted for the six-hourly CCMP product and the spectrum power within diurnal frequency band was integrated and used as a measure of variability in diurnal frequency band. More specifically, the variability within diurnal frequency band is computed as

$$V_{diurnal} = \int_{\omega_2}^{\omega_1} P(\omega) d\omega \quad (2)$$

in which ω_1 is $1/30 \text{ hr}^{-1}$ and $\omega_2 = 1/18 \text{ hr}^{-1}$ and $P(\omega)$ is the result from spectrum analysis.

Figure 5 shows the variability of wind speed at diurnal frequency band as defined in equation (2). The regions with high variability ($> 1 \text{ m}^2 \text{ s}^{-2}$) are located around coast regions and associated with land-sea breeze, such as Australia, Gulf of Mexico, Africa coast, Madagascar, north and south American coast. In the open ocean, the variance is generally around $0.1\text{-}0.2 \text{ m}^2 \text{ s}^{-2}$, which is equivalent to a change of wind speed around $0.3\text{-}0.7 \text{ m s}^{-1}$. The precipitation regions, ITCZ and SPCZ, have a slightly higher variability around $0.2\text{-}0.3 \text{ m}^2 \text{ s}^{-2}$. The diurnal variability center at the central part of subtropical high, which is not analyzed extensively, has a variance larger than $1 \text{ m}^2 \text{ s}^{-2}$. During the boreal winter time, the position of subtropical high in Northern Hemisphere moves southward, the center of large wind diurnal variability is around 30N. During boreal summer time, similar feature is evident along 30S. Associated with wind variability, the variability of surface wind convergence field also has diurnal variability (Fig. 6). Large regions of divergence is still the coastal regions. The precipitation regions are clearly visible. The central part of subtropical high is still the region of large variability.

4 Summary

The fidelity of CCMP product is assessed by comparing hourly observation and CCMP product. The Root Mean Square Difference of wind between mooring observation and CCMP product is generally around $1\text{-}2 \text{ m s}^{-1}$, or about 30% of the total wind speed, and the correlation coefficients between CCMP and mooring observations are generally high, around 0.95, which represents the current status of the best estimate of ocean surface wind by combining satellite observation and meteorological analysis field. In precipitation regions, such as ITCZ, SPCZ, and the eastern

Indian Ocean, the RMSD of wind is generally higher. Discrepancies between CCMP wind and mooring observations tend to be larger during precipitating periods. With the future launch of CYGNSS mission, it is expected that the use of L-band instrument on board CYGNSS mission can further improve the accuracy of ocean surface wind observation and alleviate the issue. Regions of large wind variability at diurnal frequency band is the coast regions and the central part of subtropical highs. The ITCZ and SPCZ regions also show up clearly in the diurnal cycle of surface wind and its convergence field.

Acknowledgments

The research was supported by NASA research grant 13-WEATHER13-0027. Technical discussion with Drs. Yuchan Yi and Andrew O'Brien are greatly appreciated.

References

- Atlas, R., R.N. Hoffman, S.C. Bloom, J.C. Jusem, and J. Ardizzone, A multiyear global surface wind velocity dataset using SSM/I wind observations. *BAMS*, 77, 5, 869 – 882, 1996.
- Bourles, B., R. Lumpkin, M.J. McPhaden, F. Hernandez, P. Nobre, E. Campos, L. Yu, S. Planton, A. Busalacchi, A.D. Moura, J. Servain, and J. Trotte, The PIRATA Program: History, Accomplishments, and Future Directions. *Bull. Amer. Meteor. Soc.*, 89, 1111–1125, 2008.
- Deser, C. and C. A. Smith, Diurnal and semidiurnal variations of the surface wind field over the tropical Pacific Ocean. *J. Climate*, 11, 1730–1748, 1998.
- Hoffman, R. N., M. Leidner, J. M. Henderson, R. Atlas, J. V. Ardizzone, and S. C. Bloom, A two-dimensional variational analysis method for NSCAT ambiguity removal: methodology, sensitivity, and tuning. *J. Atmos. Oceanic Technol.* 20, 585–605, 2003.
- McPhaden, M.J., A.J. Busalacchi, R. Cheney, J.R. Donguy, K.S. Gage, D. Halpern, M. Ji, P. Julian, G. Meyers, G.T. Mitchum, P.P. Niiler, J. Picaut, R.W. Reynolds, N. Smith, K. Takeuchi. The Tropical Ocean-Global Atmosphere (TOGA) observing system: A decade of progress. *J. Geophys. Res.*, 103, 14,169–14,240, 1998.
- McPhaden, M.J., G. Meyers, K. Ando, Y. Masumoto, V.S.N. Murty, M. Ravichandran, F. Syamsudin, J. Vialard, L. Yu, and W. Yu, RAMA: The Research Moored Array for African-Asian-Australian Monsoon Analysis and Prediction., *Bull. Am. Meteorol. Soc.*, 90, 459–480, 2009.
- Oh, J.-H., K.-Y. Kim, and G.-H. Lim, Impact of MJO on the diurnal cycle

of rainfall over the western Maritime Continent in the austral summer. *Clim. Dyn.*, 38, 1167-1180, doi:10.1007/s00382-011-1237-4, 2012.

Servain, J., A.J. Busalacchi, M.J. McPhaden, A.D. Moura, G. Reverdin, M. Vianna, and S.E. Zebiak, A Pilot Research Moored Array in the Tropical Atlantic (PIRATA). *Bull. Am. Meteorol. Soc.*, 79, 2019–2031, 1998.

Tian, B., D. E. Waliser, and E. J. Fetzer, Modulation of the diurnal cycle of tropical deep convective clouds by the MJO. *Geophys. Res. Lett.*, 33, L20704, doi:10.1029/2006GL027752, 2006.

Yang, G.-Y., and J. Slingo, The Diurnal cycle in the tropics, *Mon. Wea. Rev.*, 129, 784–801, 2001.

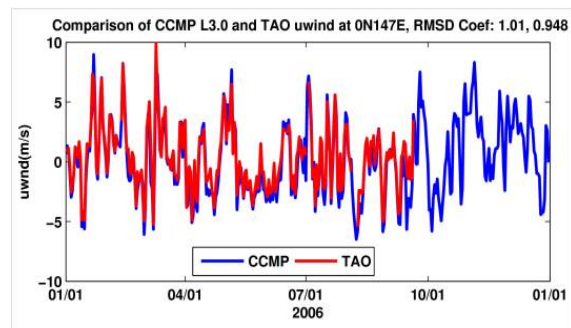


Figure 1: Comparison of hourly zonal wind from Cross-Calibrated Multi-platform Ocean Surface Wind Velocity product (CCMP) and TAO mooring observation at 0N, 147E. The root-mean-square-difference between the two is 1 m s^{-1} and the correlation coefficient is 0.95, respectively.

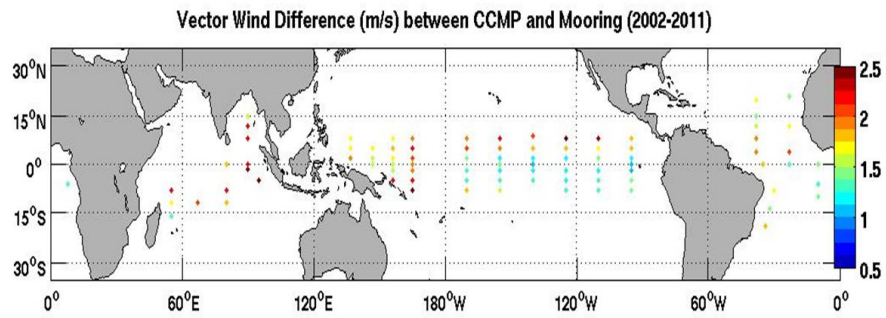


Figure 2: Root-mean-square-difference of wind between Cross-Calibrated Multiplatform Ocean Surface Wind Velocity product and mooring observation. It is the average for all available data from 2002 to 2011.

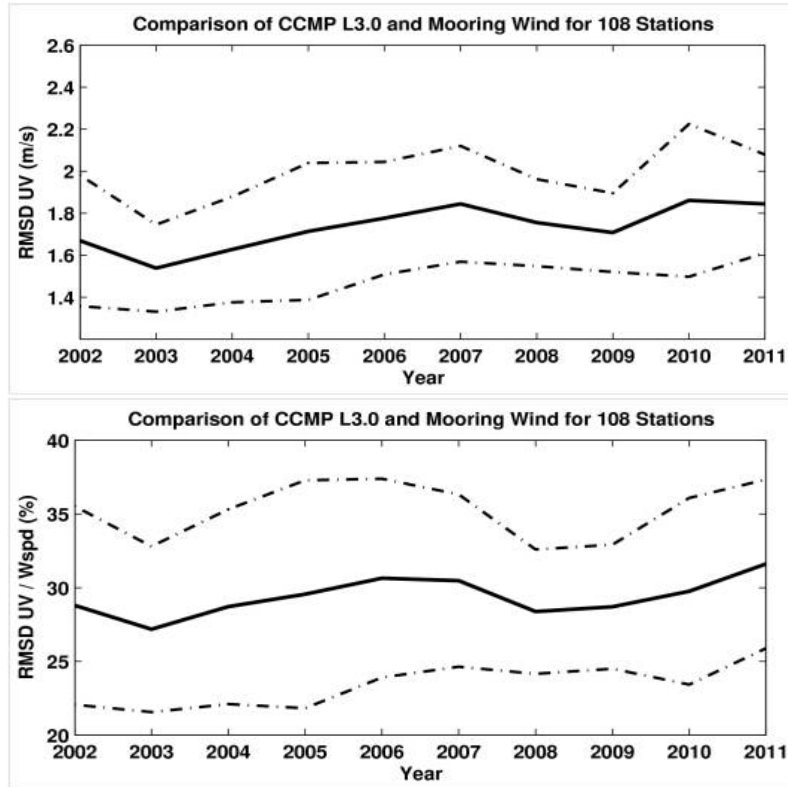


Figure 3: Time evolution of the (top) root-mean-square-difference of Cross-Calibrated Multi-platform Ocean Surface Wind Velocity product (CCMP) and mooring observation and (bottom) the ratio of the root-mean-square-difference of CCMP and mooring observation and wind speed from 2002 to 2011. It is the average for all stations for each year.

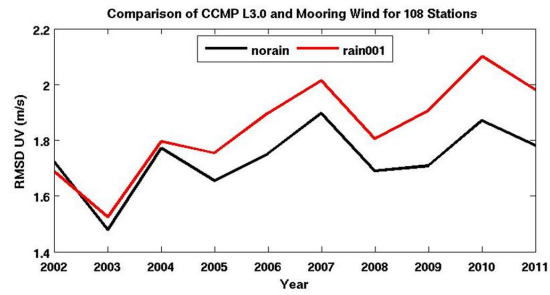


Figure 4: Comparison of RMSD of CCMP and mooring wind observation for non-precipitating (hourly rain rate smaller than 0.01 mm hr^{-1}) and precipitating (hourly rain rate larger than 0.01 mm hr^{-1}) periods.

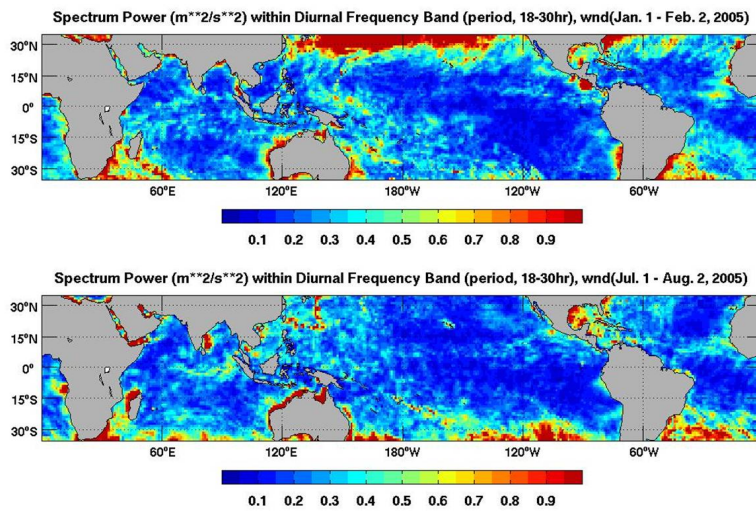


Figure 5: Variability (in unit $m^2 s^{-2}$) of surface wind speed at diurnal frequency band for January (top) and July (bottom) of 2005.

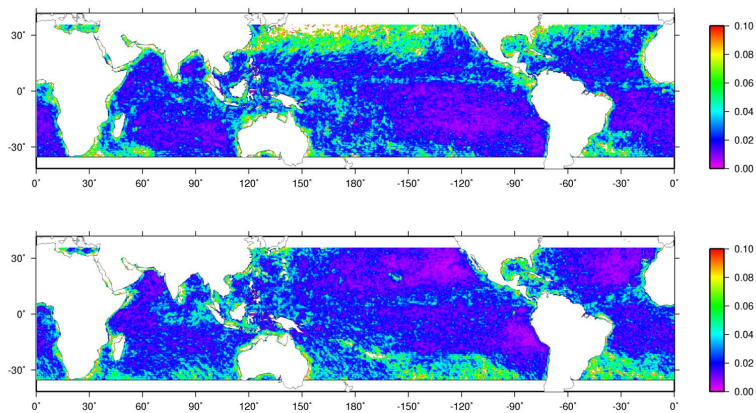


Figure 6: Variability (in unit $10^{-9}s^{-2}$) of surface wind divergence at diurnal frequency band for (top) January and (bottom) July of 2005.